Macromolecules
ARTICLE

Macromolecules **2010**, *43*, 3859–3867 **3859**
DOI: 10.1021/ma1001113

Free Volume, Transport, and Physical Properties of *n*-Alkyl Derivatized Thiol−Ene Networks: Chain Length Effect

Luke Kwisnek, Mukul Kaushik, Charles E. Hoyle, and Sergei Nazarenko*

School of Polymers and High Performance Materials, The University of Southern Mississippi, Hattiesburg, Mississippi 39406

Received January 15, 2010; Revised Manuscript Received March 3, 2010

ABSTRACT: The free volume, transport, and physical properties of a series of *n*-alkyl derivatized thiol−ene networks are reported. Derivatized thiol monomers were prepared via a nucleophile-catalyzed thio-Michael addition reaction of multifunctional thiols to *n*-alkyl acrylates ranging from $n = 1$ to $n = 16$ in length. Using UV-initiated photopolymerization, cross-linked networks were fabricated from these systematically modified thiol monomers. Each network consisted of the same molar concentration of alkyl chains. Both the thio-Michael reactions and the network photopolymerizations reached high conversion regardless of *n*-alkyl length, which is typical of the thiol−ene click reaction. The incorporation of alkyl chains led to the formation of new networks with markedly loose packing as probed by density measurements. The density decreased by 11% as n increased from 1 to 16. It is believed that the alkyl chains acted as spacers or pillars which expanded the cross-linked network scaffold increasing the free volume. The free volume behavior of these expanded networks was probed by positron annihilation lifetime spectroscopy (PALS). The hole volume size as measured by PALS doubled with an increase in alkyl chain length from 1 to 16. Oxygen transport measurements indicated an exponential increase in oxygen permeability across 2 orders of magnitude which was related to the increase in free volume. Glass transition temperatures were interestingly comparable for all derivatized networks regardless of *n*-alkyl length. Water contact angle was additionally evaluated for these derivatized networks. As expected, contact angle increased with increasing *n*-alkyl length, demonstrating that the surfaces were altered (becoming more hydrophobic) due to an increased concentration of methylene groups in the bulk.

Introduction

The incorporation of *n*-alkyl side chains of various length (up to $n = 18$) has been a common approach to polymer modification for some time. Various applications for these modified systems have been explored, such as lubricant oil and fuel viscosity modifiers,[1] modifiers to improve processing characteristics,[2−4] and temperature responsive permeation valves or barriers.[5,6] The effect of alkyl side chains has been studied almost exclusively for linear polymers.[1−6] It is interesting to discuss herein some property changes relevant to this paper and associated with the incorporation of alkyl chains of different lengths (length effect) such as T_g, contact angle, gas transport, and free volume. In general, it was observed for nearly all modified polymers (both glassy and rubbery) that T_g decreased gradually with an increase in alkyl side chain length which was attributed to increased mobility and perhaps less favorable packing associated with the presence of alkyl side chains.[7−10] Less commonly, T_g exhibited a U-shaped behavior over a similar range of alkyl side chain lengths i.e. a decrease for shorter alkyl chains followed by an increase for longer alkyl chains.[11,12] It was generally shown that gas permeability gradually increased with increasing alkyl side chain length[5,8,10,13] as long as the side chains did not crystallize in which case the permeability decreased due to the presence of impermeable crystallites.[5,6] Because permeability has been often related to free volume, the increase in permeability may be indicative of looser packing for alkyl side chain containing polymers although this effect has not been explored in great detail and free volume was not directly probed.[5,8,10,13] Finally, water contact angle was shown to increase with an increase in alkyl side chain length implying that hydrophobicity was increased as a result of a higher concentration of methylene groups to the system.[14]

In addition to linear polymer modification, attempts have been made to incorporate *n*-alkyl chains into cross-linked networks. However, only a small number of reports have been found to the best of our knowledge and they indeed caught our attention.[15−17] In two cases, *n*-alkenes up to $n = 17$ in length were incorporated (grafted) directly into flexible polymethylhydrosiloxane (PMHS) cross-linked networks.[15,16] Interestingly it was observed that the alkyl chain modified networks exhibited a noticeable increase in volume indicative of looser packing and higher free volume.[16] This effect was not explored in great detail.[16] Also cross-linked networks of chitosan were modified with *n*-alkyl chains from $n = 4$ to $n = 10$ in length.[17] An increase in protein transport was observed as alkyl chain length increased at high pH. This effect was attributed to a loose stacking of the network due to the bulky alkyl chains.[17] Finally, we were not able to identify water contact angle measurements conducted on alkyl chain modified networks.

UV-photopolymerization is an efficient and eco-friendly method of generating cross-linked networks. UV-photopolymerized thiol−ene networks in particular are known for their narrow glass transitions, low shrinkage, and 90%+ functional group conversion.[18,19] The UV-photoinitiated thiol−ene reaction, recognized as a "click" reaction,[20−22] proceeds via a step-growth free-radical process in which thiols add across double bonds (enes) in a 1:1 manner; this mechanism is reported in detail in ref 11. The thiol−ene reaction is generally conducted in the bulk

*Corresponding author. E-mail: Sergei.Nazarenko@usm.edu.

Published on Web 03/17/2010

and is uninhibited by oxygen making it a practical method for material fabrication.[18] Multifunctional thiols are reacted with multifunctional enes to yield a cross-linked network; films are generally optically clear, flexible, and robust.[18] In addition to the photoinitiated free-radical addition of a thiol to any ene, thiols also add to electron deficient enes (acrylates) via a nucleophilic catalyst, again in a 1:1 manner. This thio-Michael addition reaction has been utilized to modify surfaces,[23,24] to synthesize dendimers, stars, and oligomeric macromolecules,[25−27] and also to modify thiol monomers with different functionalities[28] including short *n*-alkyl chains up to $n = 6$ in length.[29] This reaction platform, coupled with the photopolymerization of thiol−ene networks, enabled us to conduct the current study with a focus on free volume and oxygen transport in *n*-alkyl derivatized, highly cross-linked networks.

In previous work, we reported on a series of densely cross-linked thiol−ene networks with oxygen transport properties that correlated well with T_g.[28] Oxygen permeability values spanning 3 orders of magnitude were governed by a free volume effect based on the difference between T_{test} (23 °C) and network T_g. A high barrier network was further modified with strongly interacting functional groups to demonstrate barrier improvement.[28] In this report, the same network is modified with *n*-alkyl chains from $n = 1$ to $n = 16$ in length, at constant molar concentration, with the expectation that this modification will result in a free volume increase and a decrease in barrier properties. Therefore, our intent in this work was to expand the upper range of permeabilities in basic UV-curable thiol−ene networks, which can be controlled through simple chemical derivatization of a thiol monomer.

Experimental Section

Materials. Tetrafunctional thiol monomer pentaerythritol tetrakis(3-mercaptopropionate) (4T) was supplied by Bruno Bock Thiol-Chemical-S. Trifunctional ene monomer triallyl-1,3,5-triazine-2,4,6(1*H*,3*H*,5*H*)-trione (TTT) was supplied by Sartomer. Photoinitiator α,α-dimethoxy-α-phenylacetophenone (Irgacure 651) was supplied by Ciba Specialty Chemicals. Nucleophilic catalysts diethylamine and dipropylamine were obtained from Aldrich. *N*-alkyl acrylates, from $n = 1$ to $n = 16$, were obtained as follows: Methyl acrylate, ethyl acrylate, butyl acrylate, hexyl acrylate, and lauryl acrylate ($n = 1$, 2, 4, 6, 12) were obtained from Aldrich. Octyl acrylate and decyl acrylate ($n = 8$, 10) were obtained from Monomer-Polymer and Dajac Laboratories. Tetradecyl acrylate and hexadecyl acrylate ($n = 14$, 16) were obtained from TCI America. All materials, shown in Chart 1, were used as received.

Synthesis of *n*-Alkyl Derivatized Thiol Monomers. *N*-Alkyl derivatized trifunctional thiol monomers were synthesized using a nucleophile-catalyzed thio-Michael reaction represented in Scheme 1. An example synthesis procedure for 4T derivatized with ethyl acrylate ($n = 2$) is given as follows. An amount of 4T was introduced to a round-bottom flask along with 2 mol % diethylamine. In a separate vial, an equal molar quantity of ethyl acrylate was weighed out and then added dropwise to the 4T/catalyst mixture at approximately 1 mL/min under mild stirring. The flask was then sealed and allowed to stir overnight. The resulting product, a distribution of structures which is on average a trifunctional thiol with an attached ethyl acrylate group, was not purified and used as-synthesized. This same procedure was used to synthesize modified thiol monomers with alkyl groups from $n = 1$ through $n = 14$. Hexadecyl acrylate, $n = 16$, is solid at room temperature and was melted prior to dropwise addition. Furthermore, the vessel containing the 4T/catalyst mixture was heated to 40 °C during the addition of acrylate to prevent vitrification of the 4T-16 product. Dipropylamine, at 2 mol %, was used as the nucleophilic catalyst since it is a higher-boiling amine. As in the previous procedure, the flask was sealed and allowed to stir overnight with no further purification steps.

Chart 1. Chemical Structures of Thiol and Ene Monomers, Amine Catalysts, Photoinitiator, and *n*-Alkyl Acrylate Monomers Used for Derivatization[a]

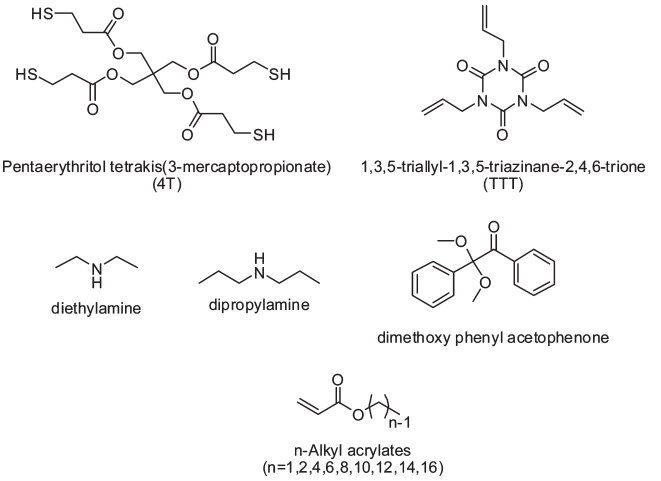

[a] $n = 1$ indicates methyl acrylate, $n = 2$ indicates ethyl acrylate, and so on.

Characterization of Products and Network Conversion. Derivatized thiol monomers were characterized by ^{1}H NMR using a Varian Mercury 200 MHz NMR spectrometer in acetone-d_6. Network conversions were characterized for samples sandwiched between two salt plates before and after UV-photopolymerization using 10 passes under a Fusion UV curing line system with a D bulb (400 W/cm^2 with belt speed of 3 m/min and 3.1 W/cm^2 irradiance). Sample thickness for IR measurements was approximately 20 μm. Change in peak area of thiol −SH groups at 2570 cm^{-1} (S−H stretch) and ene C=C groups at 3080 cm^{-1} (vinyl C−H stretch) were measured using a Bruker Tensor 37 FT-IR.

Film Formation. All of the *n*-alkyl derivatized thiol monomers were readily miscible in TTT ene monomer (1:1 molar ratio) at room temperature with only mild sonication, resulting in optically clear, homogeneous liquid mixtures. Free-standing thin films of all thiol−ene formulations were made by dissolving 1 wt % 1,1-dimethoxy-1-phenylacetophenone (Irgacure 651) photoinitiator into the thiol−ene mixture by sonication for approximately 10 min. These mixtures were then drawn down onto glass substrates using drawdown bars. The networks formed by copolymerization of the derivatized thiols with TTT are subsequently referred to by the number, n, of the carbons attached to the acrylate group: for example $n = 1$ describes a network of 4T derivatized with methyl acrylate and copolymerized with TTT, $n = 2$ describes a network of 4T derivatized with ethyl acrylate and copolymerized with TTT, and so on. In this recipe, stoichiometry of thiol, ene, and *n*-alkyl acrylate are equivalent (0.33 M each) in the final films. The basic unmodified thiol−ene network, 4T-TTT (4:3 functional group ratio meaning dangling thiol functional arms in the network), was drawn down to a thickness of approximately 0.080 mm. Remaining films were drawn-down at thicknesses ranging from 0.2 mm to 1.3 mm. This was done to ensure an adequate amount of experimental data points in the nonsteady state region of each oxygen flux curve for proper fitting. Films were cured using 10 passes under a Fusion UV curing line system with a D bulb (400 W/cm^2 with belt speed of 3 m/min and 3.1 W/cm^2 irradiance). All films were normalized in air for 3−5 days prior to testing.

Oxygen Permeation Testing. Oxygen permeation tests were conducted on Mocon OX-TRAN 2/21 instruments using a continuous-flow testing cell method approved by the ASTM (D3985). All measurements were conducted at 23 °C and 0% RH. Further details on this method were reported elsewhere.[28]

Scheme 1. Nucleophile-Catalyzed Thio-Michael Derivatization Reaction of Multifunctional Thiol with *n*-Alkyl Acrylates[a]

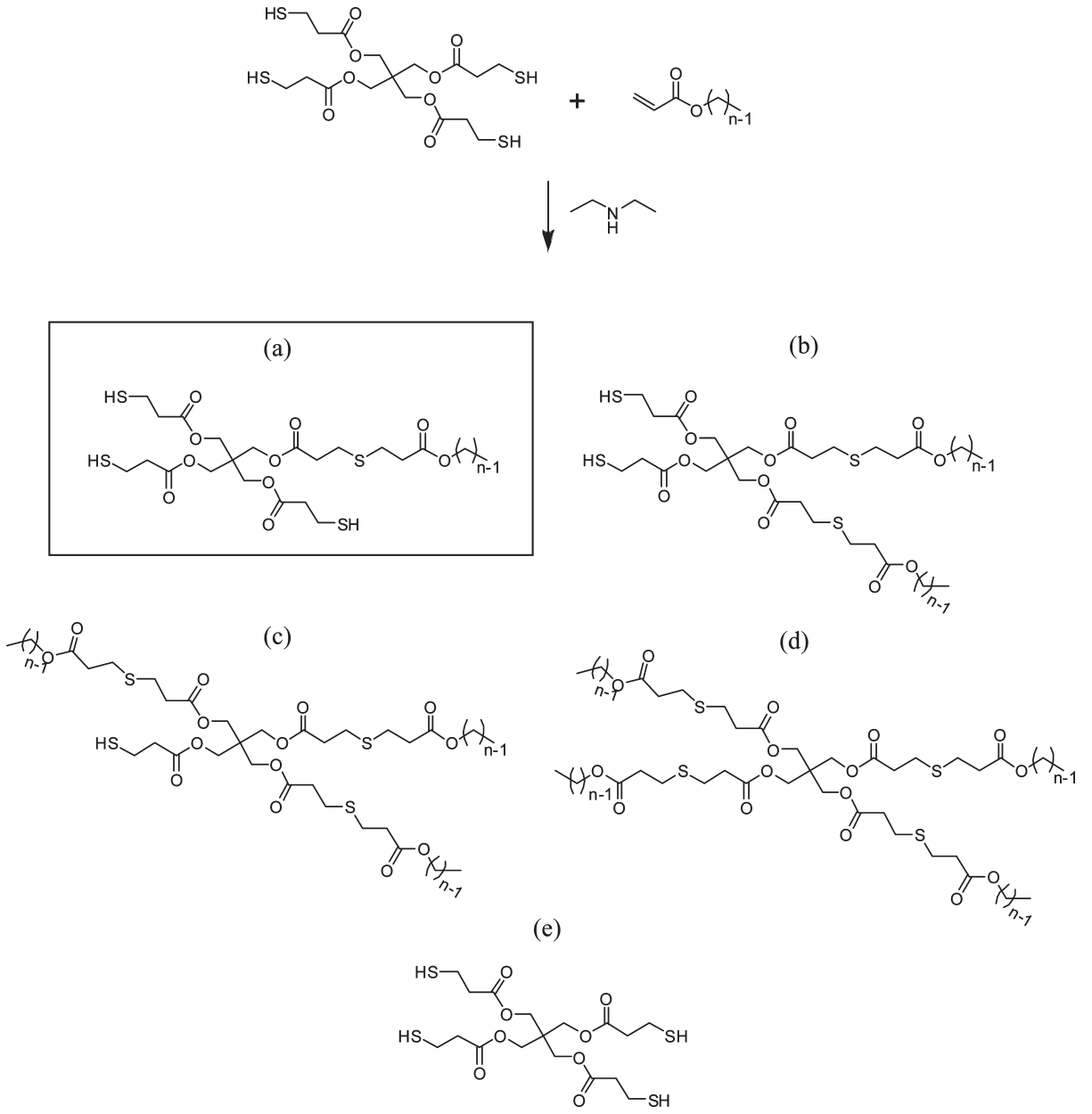

[a] Products shown are (a) an ideal trifunctional thiol with one attached alkyl chain which represents the average product and (b−e) monomers that may be present in the final mixture, a distribution of various products.

Permeability P and diffusivity D were obtained by performing a two-parameter least-squares fit of the experimental oxygen flux $J(t)$ data to Fick's second law solution (eq 1):[30]

$$J(t) = \frac{Pp}{l}\left[-\sum_{n=1}^{\infty}(-1)^n \exp(-D\pi^2 n^2 t/l^2)\right] \quad (1)$$

where p is the applied pressure and l is the film thickness. Using the solution-diffusion equation (eq 2), the solubility S was then calculated.

$$P = D \times S \quad (2)$$

Instrumentation error using this method in the range of oxygen fluxes studied is ±5% for permeability values and ±10% for diffusivity and solubility values. The remaining experimental error in obtaining P, D, and S values is largely derived from film thickness variations. For this reason, special care was taken to evaluate films of approximately uniform thickness; thickness averages were obtained by measuring at multiple locations.

Free Volume Analysis. Positron annihilation lifetime spectroscopy (PALS) is widely used in the characterization of free volume of polymers.[31,32] PALS involves measurements of the lifetime of positrons injected into a polymer sample from a positron-emitting nucleus, generally Na.[22] The lifetime (τ_3) and decay intensity (I_3) in % of the long-lived orthopositronium (positron/electron pair) o-Ps species were used to extract information about the average size of holes and general amount of free volume. The o-Ps lifetime can be related to the radius of a spherical cavity according to eq 3[33]

$$\tau_3 = \frac{1}{2}\left[1 - \frac{R}{R+d} + \frac{1}{2\pi}\sin\left(\frac{2\pi R}{R+d}\right)\right]^{-1} (ns) \quad (3)$$

where R is the average hole radius, and $d = 0.1656$ nm is the empirically determined electron layer thickness.[33] The

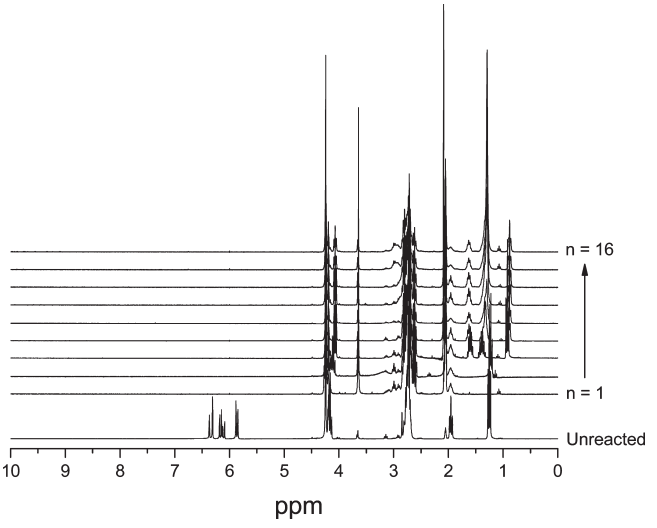

Figure 1. ^{1}H NMR spectra for *n*-alkyl derivatized thiol monomers synthesized via Scheme 1; monomers denoted by length of alkyl chain, n, where $n = 1$ is 4T + methyl acrylate, $n = 16$ is 4T + hexadecyl acrylate, etc. Disappearance of acrylate double bond proton shifts at ~6 ppm indicated successful thio-Michael derivatization. Unreacted spectrum is a mixture of 4T and ethyl acrylate without amine catalyst for comparison.

average free volume of a hole (V_h) can then be calculated as $V_h = {}^4/_3\pi R^3$.

Positron annihilation lifetime spectroscopy (PALS) experiments were conducted with a fast−fast coincidence system which is described elsewhere.[34−36] The spectrometer held two samples of approximately 1 mm thickness and 1 cm diameter with the Na^{22} positron source sandwiched between. All measurements were taken over an hour, for a total of 1×10^6 counts in each PALS spectrum. The PALS spectra were processed using PATFIT-88 software.[37] The error associated with determining τ_3 values using this software was approximately ±2%.

Miscellaneous Physical Properties. A TA Instruments Q1000 DSC with heating rate of 10 °C/min was used to investigate the glass transition temperature of film samples between 8 and 12 mg. Dynamic mechanical properties were evaluated using a Rheometric Scientific DMTA V with a frequency of 1 Hz, strain rate of 0.05%, and heating rate of 5 °C/min. T_g values were taken as the midpoint of the inflection from DSC scans and as the peak maximum in tan delta plots from DMTA. Density measurements were conducted at room temperature via the Archimedes method with a modified analytical balance and water as the buoyant fluid. Samples were film squares of approximately 1 g and masses were recorded to the third decimal place. Ambient atmosphere water contact angle measurements were conducted using a Ramé-Hart model 200−00 standard goniometer. Deionized water droplets of approximately 5 mm in diameter were applied to thin films via a 0.6 mm diameter syringe; three droplets for each film, with five measurements per drop, were recorded.

Results and Discussion

Derivatization and Network Conversion. Derivatization of thiol monomers was verified via ^{1}H NMR after reaction completion. Figure 1 shows ^{1}H NMR spectra for each modified monomer mixture. Success of the thio-Michael reaction was verified by the disappearance of the acrylate double bond proton shifts at ~6 ppm. For comparison, the ^{1}H NMR spectrum of an unreacted mixture of 4T and ethyl acrylate sans amine catalyst is shown (labeled as "unreacted"). Following NMR verification, the monomer mixtures were not purified and used as-synthesized as mentioned in the Experimental Section.

The issue of the *n*-alkyl chains interfering with functional group conversion during polymerization is a valid one, especially given that increasing *n*-alkene lengths led to decreased conversions for *n*-alkene grafting-to reactions in siloxane networks.[15,16] To address this concern, IR measurements were conducted on liquid monomer mixtures (before curing) and cured networks (after curing) as detailed in the Experimental Section. Figure 2 shows the peak areas for thiol (~2570 cm^{-1}) and ene (~3080 cm^{-1}) functional groups before and after UV curing for three networks. These three spectra are representative of the entire series of *n*-alkyl derivatized thiol−ene networks. It is evident that high conversions are reached for each network; *n*-alkyl chain length has no measurable effect on the ultimate conversion of thiol and ene groups during photoinitiated polymerization. Note that the prepolymerization monomer derivatization technique used in this work is advantageous especially in the case of forming a cross-linked network − the network conversions are near or above 90% and the *n*-alkyl derivatization reaction is quantitative.

Transport, Free Volume, and Density. Figure 3 shows experimental oxygen flux data (open circles) versus time for three representative *n*-alkyl derivatized networks—with lengths $n = 1$, 4, and 16. All dependencies exhibited non-steady state and steady-state portions of permeation, suggestive of complete sample degassing prior to testing as mentioned in the Experimental section. Solid lines are the fits to eq 1. The fit was excellent in each case, indicative of Fickian behavior. The sample with $n = 1$ showed the smallest steady-state flux while the sample with $n = 16$ the largest steady-state flux, despite that it had a much greater thickness. The excellent fits allowed the accurate decoupling of the diffusivity *D*, and solubility, *S*, terms of the permeability, *P*, for all networks. Individual *P*, *D*, and *S* values for all modified networks are shown in Table 1. In addition, we report data for the unmodified thiol−ene network which was prepared using unmodified 4T and TTT monomers as described in the Experimental Section. The basic, unmodified thiol−ene network exhibited the smallest average hole free volume size, lowest oxygen permeability, and lowest oxygen diffusivity as reported in Table 1 as well as the highest T_g as seen in Figures 10−13. From this point onward, we will analyze and compare materials within the *n*-alkyl derivatized family of networks. However, the values for unmodified network are included on each corresponding figure.

For convenience, oxygen permeability and diffusivity for the *n*-alkyl derivatized networks are plotted logarithmically as a function of n, the alkyl chain length, in Figure 4. From $n = 1$ to $n = 16$, there is a gradual increase in both *P* and *D*. Particularly, permeability increases by 2 orders of magnitude while diffusivity increases by approximately 1 order of magnitude. However there appears to be a tendency for both *P* and *D* to level off across the series approaching a plateau at $n = 16$.

Oxygen solubility values also show a strong increase with increasing length of the alkyl chain as plotted linearly in Figure 5. Solubility values nearly quadrupled across the series of *n*-alkyl derivatized networks and also appear to level off in a fashion similar to *P* and *D*. Therefore, both *D* and *S* make a comparable contribution to the increases in permeability, *P*. To further substantiate these transport results and because both *D* and *S* are often related to free volume, hole free volume was investigated via PALS.

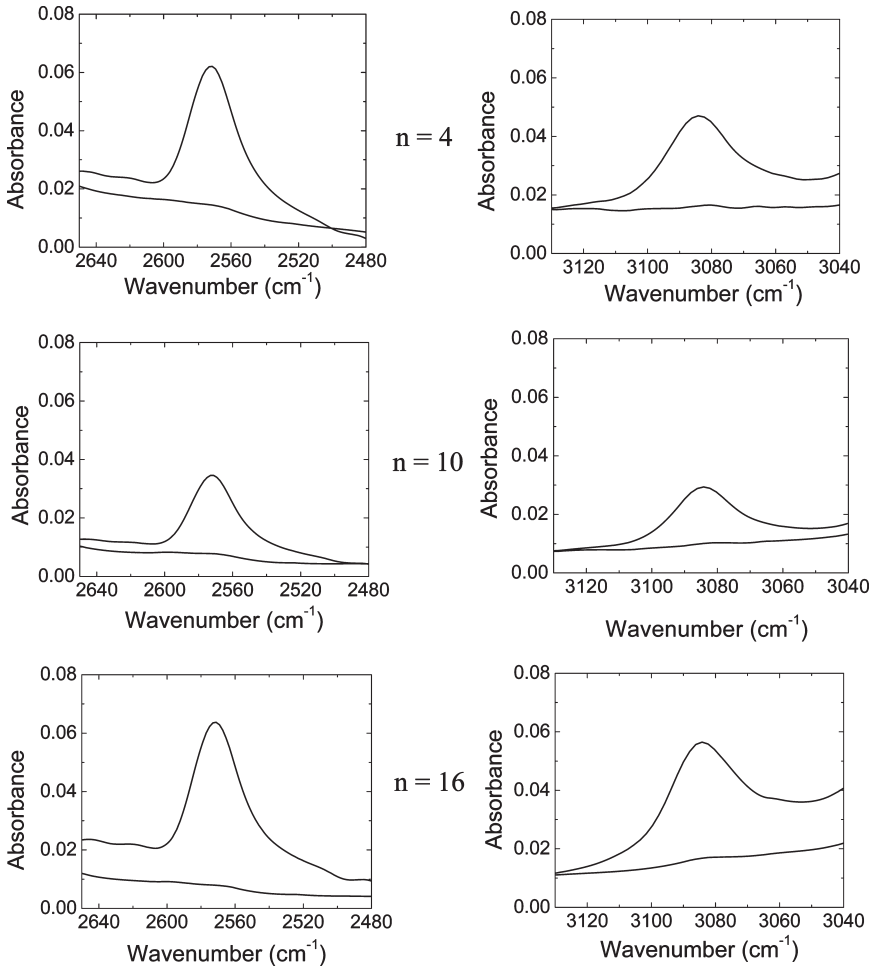

Figure 2. FTIR spectra of the thiol (2570 cm^{-1}) peaks and ene (3080 cm^{-1}) peaks before and after UV-initiated polymerization for three representative *n*-alkyl derivatized thiol−ene networks. Labels indicate length of alkyl chain in the network. High conversions are obtained for each network including those not shown.

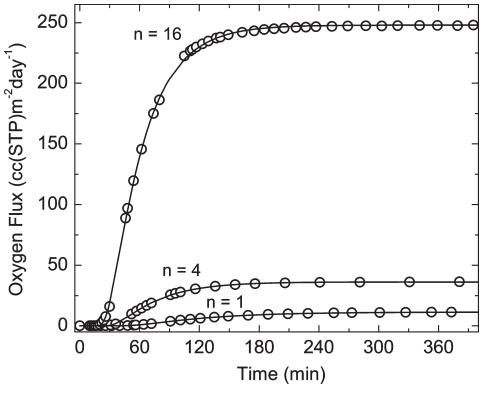

Figure 3. Representative experimental oxygen flux data (circles) and fit to eq 1 (lines) for *n*-alkyl derivatized thiol−ene networks where $n = 1$ (thickness = 0.22 mm), $n = 4$ (thickness = 0.30 mm), and $n = 16$ (thickness = 0.80 mm).

Free volume models are broadly used to interpret gas transport data especially in the rubbery state. Mean hole free volume, $\langle V_h \rangle$, is shown as a function of the alkyl chain length in Figure 6 with actual values listed in Table 1. An increase in hole free volume size across the series was apparent. From $n = 1$ to $n = 16$, the extremes, V_h doubled. This increase in free volume also manifests as sizable bulk dedensification shown as a separate plot in Figure 6 (right axis). Over the range of alkyl chain lengths studied, the density of the networks decreased by about 11%. This decrease in density is particularly interesting since the increased bulkiness overcomes the increase in mass associated with alkyl chains of increasing length (longer chain has more methylene groups, i.e. more mass). A small unit of network is thus increased in volume more than is indicated by the density measurements alone.

Often an increase in free volume especially in the rubbery state is attributed to a chain end effect. Considering the same unit as defined in the previous paragraph, the number of chain ends would be the same per unit however the volume concentration naturally would be reduced implying that a chain end effect cannot be responsible for this free volume behavior.

Instead it is believed that the alkyl chains act as spacers or pillars which expand the cross-linked network scaffold increasing free volume. This possibility has been considered elsewhere for linear polymers.[2−4] The rigidity or bulkiness of fairly short alkyl chains can be somewhat understood from the fact that short chains may not follow Gaussian chain statistics and this may lead to an overall chain configuration enriched with trans conformations. It is anticipated that this effect will be less dramatic as n increases further beyond a certain limit leading to a leveling off of this expansion effect. Figure 7 represents graphically the explanation related to our system where free volume increase is associated with the separation of the network scaffold by alkyl chains. Thus, the expansion of the network scaffold due to the bulkiness of

Table 1. Oxygen Transport Data, Recorded at 23 °C, and Free Volume Data, Recorded at Ambient Room Temperature

material (*n*-alkyl length)	oxygen permeability (cm^3(STP) cm m^{-1} day^{-1} atm^{-1})	oxygen diffusivity (cm^2 s^{-1})	oxygen solubility (cm^3(STP) $cm^{-3}atm^{-1}$)	V_h (Å^3)	I_3 (%)
unmodified	0.041	1.7×10^{-9}	0.026	63	14.7
1	0.25	1.2×10^{-8}	0.025	83	15.1
2	0.39	1.8×10^{-8}	0.024	84	15.8
4	1.1	3.8×10^{-8}	0.033	101	15.3
6	2.1	6.3×10^{-8}	0.038	113	16.1
8	2.9	7.1×10^{-8}	0.047	125	16.5
10	4.7	9.5×10^{-8}	0.057	139	15.1
12	7.3	1.4×10^{-7}	0.060	154	16.2
14	14.3	2.9×10^{-7}	0.057	161	15.7
16	19.7	3.3×10^{-7}	0.070	164	15.5

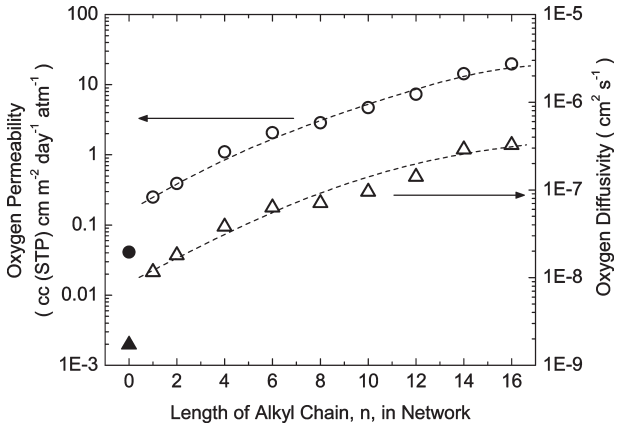

Figure 4. Oxygen permeability (circles) and diffusivity (triangles) as a function of n, the length of alkyl chain in the thiol−ene network. Filled symbols are data for unmodified thiol−ene network.

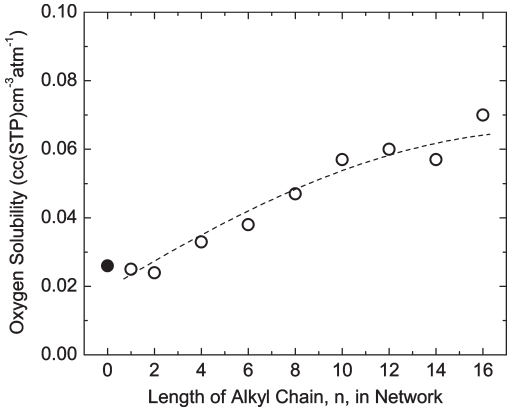

Figure 5. Oxygen solubility as a function of alkyl chain length. Unmodified thiol−ene network shown as filled symbol.

alkyl chains is a plausible explanation for the free volume increase and concomitant dedensification in the derivatized thiol−ene networks reported here.

A question can be raised regarding nanophase separation (aggregation) of hydrophobic alkyl chains. This effect was previously identified for linear polymers with flexible backbones;[7] however, we believe that this scenario is unlikely due to topological restrictions imposed by the cross-linked network assuming that alkyl chains are incorporated randomly. Nanophase separation may occur prior to network formation, and this possibility cannot be completely ruled out although it is not exactly clear to what extent this behavior could be related to dedensification.

It is worthwhile to discuss a more quantitative correlation between free volume and transport. The general relationship

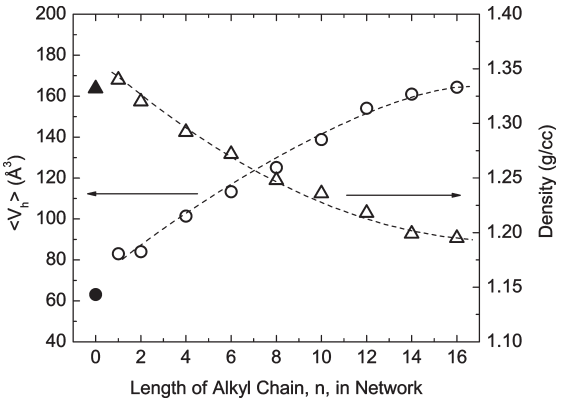

Figure 6. Mean hole free volume, $\langle V_h \rangle$ (circles), and film density (triangles) as a function of alkyl chain length. Unmodified thiol−ene network shown as filled symbols.

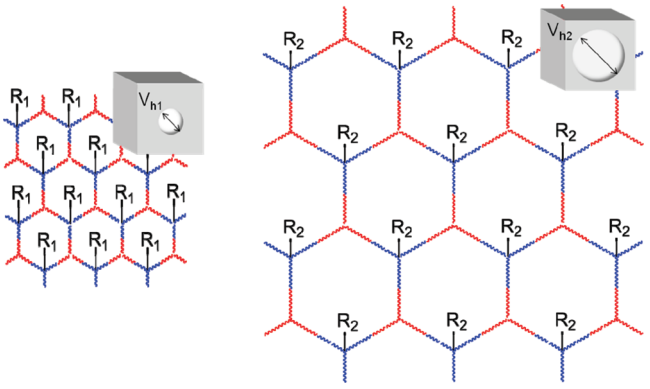

Figure 7. Idealized, two-dimensional lattice-like schematic illustrating expansion of network scaffold with increasing alkyl chain length ($R_2 > R_1$). Also shown are representative three-dimensional network sections demonstrating increased free volume hole size ($V_{h2} > V_{h1}$) corresponding to this network expansion.

between hole free volume and gas diffusivity can be explicitly expressed using the generalized eq 4 as follows:

$$D = Ae^{(-B/V_h)} \tag{4}$$

where D is the diffusion coefficient, A and B are constants, and V_h is the hole free volume.[38] This relationship was shown to be valid when the free volume term is either hole free volume[39−43] or fractional free volume.[44−47] The intensity, I_3, has been related to the concentration of holes[39] however this intensity is constant for all derivatized networks as shown in Figure 8. This result shows that the number of holes is equivalent for each network.[39] Thus, mean hole free volume, $\langle V_h \rangle$, corresponds to fractional free volume, V_f,[39] and so a

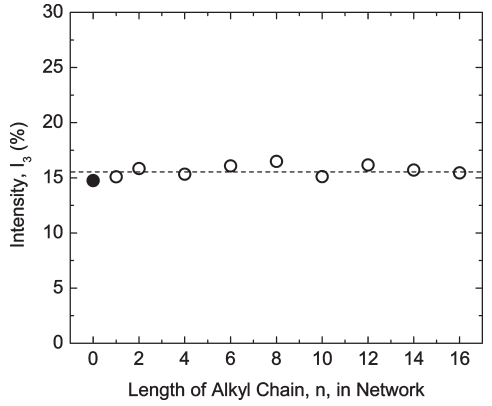

Figure 8. Intensity, I_3, of *o*-positronium as a function of alkyl chain length demonstrating constant nature of I_3 values. Unmodified thiol−ene network is shown as filled symbol.

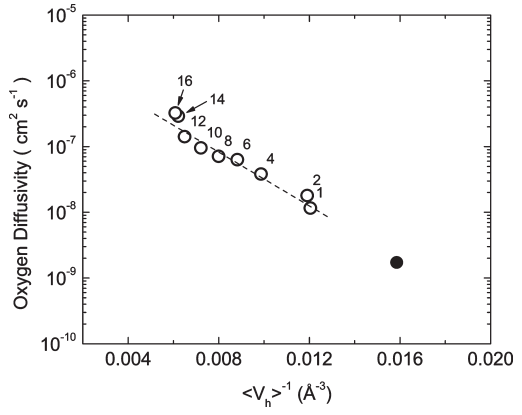

Figure 9. Relationship between oxygen diffusivity and the inverse of mean hole free volume via PALS for all networks. *n*-Alkyl derivatized networks denoted by the length of alkyl chain, *n*. Unmodified network shown as filled symbol.

plot of log(D) vs $1/\langle V_h \rangle$ should elucidate the general free volume dependency of gas diffusivity for the *n*-alkyl derivatized thiol−ene networks as shown in Figure 9. There appears to be a satisfactory correlation between log(D) and $1/\langle V_h \rangle$ in this case. This correlation, likely due to the homologous nature of this series of materials and in agreement with the oxygen transport results, is indicated by the dashed line. It is evident that hole free volume is one of the governing factors for oxygen transport in this series of networks.

Hole free volume can also be related to specific volume (V_{sp}) via eq 5:[48]

$$V_{sp} = V_{occ} + N_h V_h \quad (5)$$

where V_{occ} is the specific occupied volume, which includes van der Waals and interstitial free volumes, and N_h is the number of holes per gram of polymer. Traditionally, specific volume data derived from pressure-volume-temperature (*PVT*) measurements have been combined with hole free volume from PALS temperature scan measurements to calculate N_h and V_{occ}.[48,49] In this work, a similar correlation can be made however using density and PALS measurements at room temperature from the systematic variation in the alkyl chain length within the network instead of temperature data. This correlation is shown in Figure 10 for the alkyl chain derivatized thiol−ene networks. An excellent linear fit of the experimental data was achieved. This excellent fit of the experimental data at room temperature for the thiol−ene

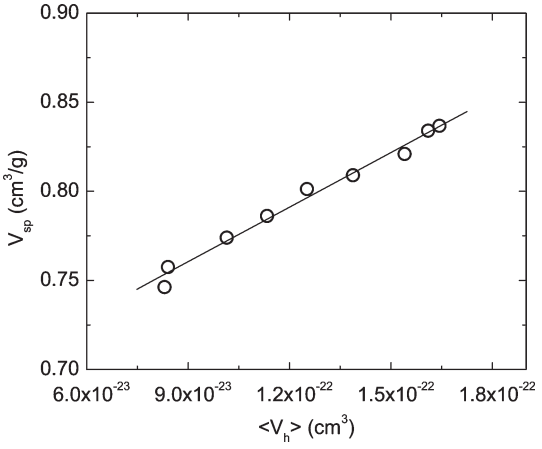

Figure 10. Correlation between specific volume (V_{sp}) and average hole free volume (V_h) for measurements conducted at room temperature while varying the length of the alkyl chain, *n*, in the thiol−ene network.

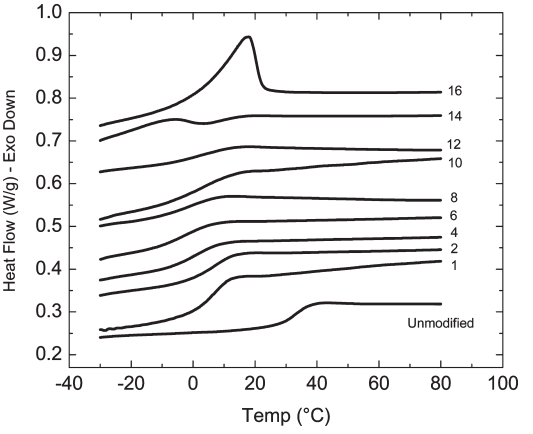

Figure 11. DSC 2nd heating scans for *n*-alkyl derivatized thiol−ene networks. Labels denote length of alkyl chain in network.

networks indicates that N_h is relatively constant for each network regardless of the alkyl chain length. This result is in agreement with the fact that I_3, which has been related to the concentration of holes, is also constant.[39] Using eq 5, $V_{occ} = 0.668 \pm 0.005$ cm^3/g and $N_h = 10.21 \pm 0.46 \times 10^{20}$ holes/g. The range of N_h previously reported for different polymeric systems varied from about 2×10^{20} to 9×10^{20} holes/g.[50,51] Therefore, N_h found for the alkyl chain modified thiol−ene networks is reasonable though somewhat on the high end. We also speculate that N_h values from *PVT* and PALS temperature measurements would be in agreement with N_h calculated via the method reported here although this is currently being investigated.

Glass Transition and Surface Tension. The length of alkyl side chains can have a profound effect on T_g in linear and lightly cross-linked polymers as mentioned in the Introduction. It was beneficial to explore this effect for the family of *n*-alkyl derivatized thiol−ene networks. Experimental DSC scans are provided in Figure 11 and experimental DMTA tan δ and storage modulus (E') plots are provided in Figure 12 for the *n*-alkyl derivatized thiol−ene networks. T_g values as a function of alkyl chain length are shown in Figure 13. The *n*-alkyl derivatized thiol−ene networks show a slight decrease followed by a slight increase in T_g via DMTA as n increases; this behavior is consistent with certain reports on linear polymers.[11,12] Glass transitions by DSC, which are only available for $n = 1$ to 12 due to crystalline melting peaks

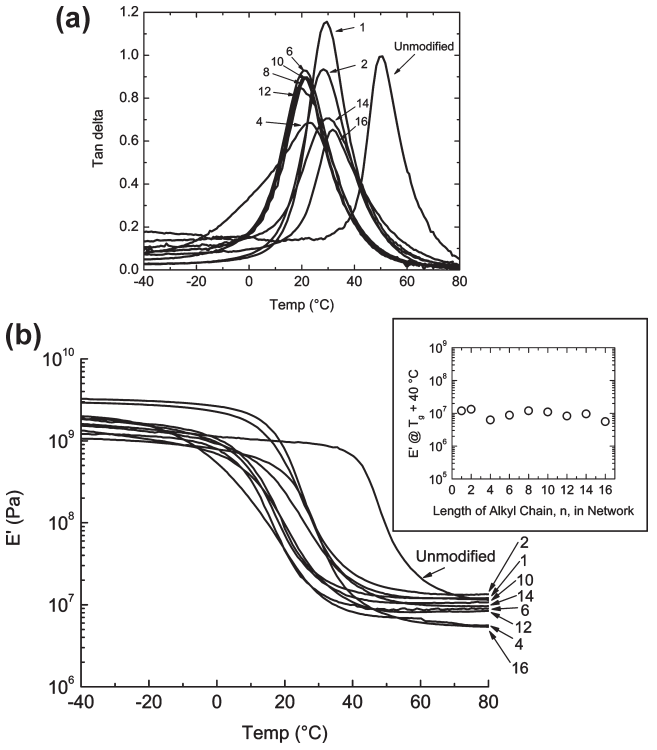

Figure 12. (a) DMTA tan δ plots and (b) DMTA E' plots for *n*-alkyl derivatized thiol−ene networks. Labels denote length of alkyl chain in network.

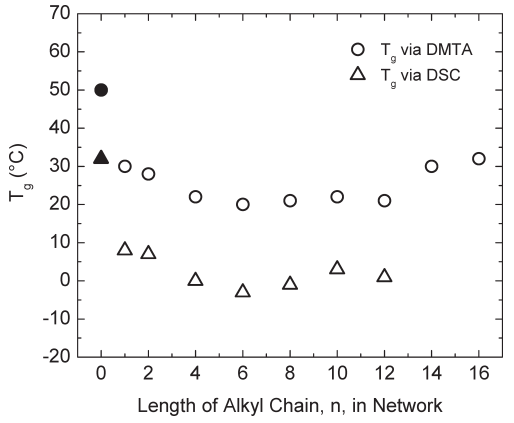

Figure 13. Glass transition temperatures via DSC and DMTA. Unmodified thiol−ene network indicated as filled symbols.

that appear in the transition region at higher n, are in agreement with DMTA results albeit they are all lower than the DMTA values which is expected. However the change in T_g for the *n*-alkyl derivatized thiol−ene networks is within a 10 °C window for both DSC and DMTA methods, indicating that the alkyl chains in the cross-linked network do not strongly affect the glass transition. Since these are cross-linked networks, mobility and relaxation modes are restricted as compared to linear polymers. The glass transition appears to be controlled mainly by the rigidity of the thiol and ene monomers that make up the network scaffold and is not so much influenced by the increasing *n*-alkyl length. Although free volume can be related to T_g as we have done in the past for basic thiol−ene networks of varying structure and rigidity,[28] this is not the case for the *n*-alkyl derivatized networks which consist of an identical network scaffold. Perhaps this methodology may be applied to other networks

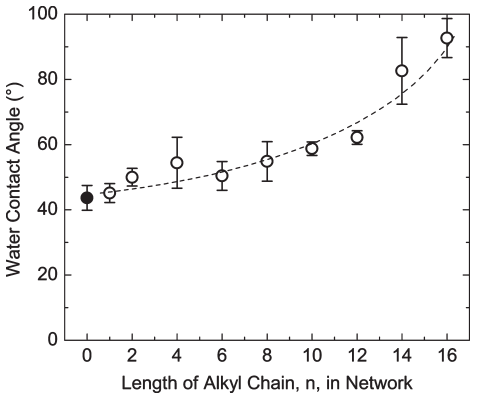

Figure 14. Water contact angle as a function of alkyl chain length. Filled symbol is unmodified thiol−ene network.

to maintain a similar T_g but vastly increase the free volume. Shown also in Figure 12b are E' plots for the *n*-alkyl derivatized network. Rubbery modulus values at T_g + 40 °C as a function of alkyl chain length are shown as an inset on this figure. These moduli were within a window of about a factor of 2 and no readily apparent trend was observed. This result suggests that the cross-link density, upon which the rubbery modulus is dependent, is not measurably influenced by the presence or the length of the alkyl chains for this series of thiol−ene networks. Furthermore, note that there is no crystallinity at the testing temperature (23 °C) in any of the networks.

Since increasing alkyl chain length brings about compositional changes in the thiol−ene networks, i.e. an increasing concentration of hydrocarbon moieties, it is worthwhile to discuss surface tension as a function of increasing alkyl chain length. Water contact angle measurements on the *n*-alkyl derivatized thiol−ene networks showed increasing contact angle as n increases according to Figure 14. As expected, the most hydrophobic behavior was observed for the $n = 16$ derivatized network which is indicative of the highest number of methylene groups per structural network unit. Summarizing, it is apparent that the *n*-alkyl chains modify the surface energy of the thiol−ene networks in agreement with results for linear *n*-alkyl (meth)acrylates.[14]

Conclusions

N-Alkyl modified thiol−ene networks, from $n = 1$ to $n = 16$ in alkyl chain length, were fabricated by photopolymerizing *n*-alkyl acrylate-derivatized multifunctional thiol monomers with a conventional trifunctional ene monomer. High functional group conversions for both the thio-Michael derivatization reaction and the network photopolymerizations were achieved for all lengths of n. Free volume increased greatly as alkyl chain length increased, doubling in magnitude from $n = 1$ to $n = 16$. The free volume increase was verified by bulk density measurements which revealed significant dedensification as a result of increasing alkyl chain length. As a result of the free volume increase, oxygen permeability, diffusivity, and solubility each increased. It was proposed that the covalently bound alkyl chains acted as pillars or spacers expanding the free volume. T_g of the *n*-alkyl derivatized networks were relatively constant, remaining in a window of 10 °C. Lastly, surface energy was also greatly influenced as evidenced by water contact angle measurements, leading to hydrophobic behavior at longer alkyl chain lengths. Furthermore, this report demonstrates the ease of tuning and forming cross-linked networks at room temperature in the bulk using thiol−ene click chemistry as well as the significant property variations that were observed in these systematically modified materials. Present work is aimed at incorporating

fluoroalkyl chains into the network as well as measuring CO_2 and N_2 transport for potential membrane applications. Additionally, *PVT* and PALS temperature sweep measurements are underway with the goal of comparing N_h values from temperature data with those from varying the length of the alkyl chain as presented in this work.

Acknowledgment. The authors acknowledge Fusion UV Systems for the light source and financial support of this project and Bruno Bock, Sartomer, and Ciba Specialty Chemicals for materials.

Note Added after ASAP Publication. This article posted ASAP on March 17, 2010. Due to a production error, figure 11 appeared incorrectly. The correct version posted on March 30, 2010.

References and Notes

(1) Jordan, E. F., Jr.; Smith, S., Jr.; Koos, R. E.; Barker, W. F.; Artymyshyn, B.; Wrigley, A. N. *J. Appl. Polym. Sci.* **1978**, *22*, 1509.
(2) Qiao, X.; Wang, X.; Mo, Z. *Synth. Met.* **2001**, *118*, 89.
(3) Hsu, W.-P.; Levon, K.; Ho, K.-S.; Myerson, A. S.; Kwei, T. K. *Macromolecules* **1993**, *26*, 1318.
(4) Lee, C.; Kim, K. J.; Rhee, S. B. *Synth. Met.* **1995**, *65*, 295.
(5) Mogri, Z.; Paul, D. R. *Polymer* **2001**, *42*, 7765.
(6) Kirkland, B. S.; Paul, D. R. *Polymer* **2008**, *49*, 507.
(7) Beiner, M. *Macromol. Rapid Commun.* **2001**, *22*, 869.
(8) Pinnau, I.; Morisato, A.; He, Z. *Macromolecules* **2004**, *37*, 2823.
(9) Dorkenoo, D. K.; Pfromm, P. H.; Rezac, M. E. *J. Polym. Sci., Part B: Polym. Phys.* **1998**, *36*, 797.
(10) Matsumoto, A.; Oki, Y.; Otsu, T. *Polym. J.* **1991**, *23*, 201.
(11) Wisian-Neilson, P.; Bailey, L.; Bahadur, M. *Macromolecules* **1994**, *27*, 7713.
(12) Overberger, C. G.; Frazier, C.; Mandelman, J.; Smith, H. F. *J. Am. Chem. Soc.* **1953**, *75*, 3326.
(13) Wisian-Neilson, P.; Xu, G. *Macromolecules* **1996**, *29*, 3457.
(14) Clarke, M. L.; Chen, C.; Wang, J.; Chen, Z. *Langmuir* **2006**, *22*, 8800.
(15) Mukbaniani, O.; Titvinidze, G.; Tatrishvili, T.; Mukbaniani, N.; Brostow, W.; Pietkiewicz, D. *J. Appl. Polym. Sci.* **2007**, *104*, 1176.
(16) Thami, T.; Nasr, G.; Bestal, H.; van der Lee, A.; Bresson, B. *J. Polym. Sci., Part A: Polym. Chem.* **2008**, *46*, 3546.
(17) Li, F.; Liu, W. G.; Yao, K. D. *Biomaterials* **2002**, *23*, 343.
(18) Hoyle, C. E.; Lee, T. Y.; Roper, T. *J. Polym. Sci., Part A: Polym. Chem.* **2004**, *42*, 5301.
(19) Jacobine, A. F. In *Radiation Curing in Polymer Science and Technology*; Fouassier, J. P., Rabek, J. F., Eds.; Elsevier Applied Science: London, 1993; Vol. *III*, pp 219−268.
(20) Becer, C. R.; Hoogenboom, R.; Schubert, U. S. *Angew. Chem., Int. Ed.* **2009**, *48*, 2.
(21) Iha, R. K.; Wooley, K. L.; Nystrom, A. M.; Burke, D. J.; Kade, M. J.; Hawker, C. *J. Chem. Rev.* **2009**, *109*, 5620.
(22) Sumerlin, B. S.; Vogt, A. P. *Macromolecules* **2010**, *43*, 1.
(23) Khire, V. S.; Benoit, D. S. W.; Anset, K. S.; Bowman, C. N. *J. Polym. Sci., Part A: Polym. Chem.* **2006**, *44*, 7027.
(24) Khire, V. S.; Lee, T. Y.; Bowman, C. N. *Macromolecules* **2007**, *40*, 5669–5677.
(25) Clark, T.; Kwisnek, L.; Hoyle, C. E.; Nazarenko, S. *J. Polym. Sci., Part A: Polym. Chem.* **2009**, *47*, 14.
(26) Chan, J. W.; Yu, B.; Hoyle, C. E.; Lowe, A. B. *Polymer* **2009**, *50*, 3158.
(27) Chan, J. W.; Hoyle, C. E.; Lowe, A. B. *J. Am. Chem. Soc.* **2009**, *131*, 5751.
(28) Kwisnek, L.; Nazarenko, S.; Hoyle, C. E. *Macromolecules* **2009**, *42*, 7031.
(29) Shin, J.; Nazarenko, S.; Hoyle, C. E. *Macromolecules* **2009**, *42*, 6549.
(30) Hiltner, A.; Liu, R. Y. F.; Baer, E. *J. Polym. Sci., Part B: Polym. Phys.* **2005**, *43*, 1047.
(31) Schrader, D. M.; Jean, Y. C., Eds. *Positron and and Positron Chemistry*: Elsevier: Amsterdam, 1988.
(32) Pethrick, R. A. *Prog. Polym. Sci.* **1997**, *22*, 1.
(33) Tao, S. J. *J. Chem. Phys.* **1972**, *56*, 5499.
(34) Kobayashi, Y.; Zheng, W.; Meyer, E. F.; McGervey, J. D.; Jamieson, A. M. *Macromolecules* **1989**, *22*, 2302.
(35) Kluin, J. E.; Yu, Z.; Vleeshouwers, S.; McGervey, J. D.; Jamieson, A. M.; Simha, R. *Macromolecules* **1993**, *26*, 1853.
(36) Chang, G. W.; Yu, Z.; Jamieson, A. M.; McGervey, J. D. *J. Appl. Polym. Sci.* **1997**, *63*, 483.
(37) Kirkegard, P.; Eldrup, M.; Morgesen, O. E.; Pedersen, N. J. *Comput. Phys. Commun.* **1981**, *23*, 307.
(38) Cohen, M. H.; Turnbull, D. *J. Chem. Phys.* **1959**, *31*, 1164.
(39) Ito, K.; Saito, Y.; Yamamoto, T.; Ujihira, Y.; Nomura, K. *Macromolecules* **2001**, *34*, 6153.
(40) Park, J. Y.; Paul, D. R. *J. Membr. Sci.* **1997**, *125*, 23.
(41) Hill, A. J.; Weinhold, S.; Stack, G. M.; Tant, M. R. *Eur. Polym. J.* **1996**, *32*, 843.
(42) Tanaka, K.; Kawai, T.; Kita, H.; Okamoto, K.; Ito, Y. *Macromolecules* **2000**, *33*, 5513.
(43) Nagel, C.; Gunther-Schade, K.; Fritsch, D.; Strunskus, T.; Faupel, F. *Macromolecules* **2002**, *35*, 2071.
(44) Hu, Y. S.; Liu, R. Y. F.; Zhang, L. Q.; Rogunova, M.; Schiraldi, D. A.; Nazarenko, S.; Hiltner, A.; Baer, E. *Macromolecules* **2002**, *35*, 7326.
(45) Ponangi, R.; Pintauro, P. N.; De Kee, D. *J. Membr. Sci.* **2000**, *178*, 151.
(46) Villaluenga, J. P. G.; Seoane, B.; Compan, V. *J. Appl. Polym. Sci.* **1998**, *70*, 23.
(47) Tanaka, K.; Kita, H.; Okano, M.; Okamoto, K. *Polymer* **1992**, *33*, 585.
(48) Dlubek, G.; Stejny, J.; Alam, M. A. *Macromolecules* **1998**, *31*, 4574.
(49) Kilburn, D.; Bamford, D.; Dlubek, G.; Pionteck, J.; Alam, M. A. *J. Polym. Sci., Part B: Polym. Phys.* **2003**, *41*, 3089.
(50) Goyanes, S.; Rubiolo, G.; Marzocca, A.; Salgueiro, W.; Somoza, A.; Consolati, G.; Mondragon, I. *Polymer* **2003**, *44*, 3193.
(51) Dlubek, G.; Pionteck, J.; Sniegocka, M.; Hassan, E. M.; Krause-Rehberg, R. *J. Polym. Sci., Part B: Polym. Phys.* **2007**, *45*, 2519.